May, 2006

In Situ Sum Frequency Generation Vibrational Spectroscopy Observation of a Reactive Surface Intermediate during High-Pressure Benzene Hydrogenation

Kaitlin M. Bratlie, *University of California - Berkeley*
Lucio D. Flores, *University of California - Berkeley*
Gabor A. Somorjai, *University of California - Berkeley*

In Situ Sum Frequency Generation Vibrational Spectroscopy Observation of a Reactive Surface Intermediate during High-Pressure Benzene Hydrogenation

Kaitlin M. Bratlie, Lucio D. Flores, and Gabor A. Somorjai*

Department of Chemistry, University of California, Berkeley, California 94720, and Materials Science Division, Lawrence Berkeley National Laboratory, Berkeley, California 94720

Received: February 28, 2006; In Final Form: April 6, 2006

Sum frequency generation surface vibrational spectroscopy and kinetic measurements using gas chromatography have been used to identify a reactive surface intermediate in situ during hydrogenation of benzene on a Pt(111) single crystal surface at Torr pressures. Upon adsorption at 310 K, both chemisorbed and physisorbed benzene coexist on the surface, a result which has not previously been observed. Kinetic measurements show a linear compensation effect for the production of both cyclohexane and cyclohexene. From these data the isokinetic temperature was identified and correlated to the chemisorbed benzene species, which were probed by means of vibrational spectroscopy. Additionally, chemisorbed benzene was determined to be a reactive intermediate, which is critical for hydrogenation.

1. Introduction

Catalytic reactions involving aromatic molecules are important in the chemical industry for both fuel reforming and environmental concerns.[1] To better understand industrial catalytic processes, we carry out model studies using platinum single-crystal surfaces at pressures and temperatures used in the chemical technologies. In the case of benzene hydrogenation, earlier studies have shed light on the adsorption and reaction mechanism: 1,3- as well as 1,4-cyclohexadiene, cyclohexane, and cyclohexene have been postulated as possible surface species.[2−17] The large number of possible reaction pathways (based on the surface species given above), has led to numerous studies probing adsorption and isolated reactions (hydrogenation/dehydrogenation) of these species. Despite the vast quantity of data published on these cyclic hydrocarbons, very little is known regarding the surface chemistry at ambient pressures and the nature of reactive surface intermediates. This results from a paucity of techniques that are capable of probing surface intermediates at ambient pressures.

Various surface analytical techniques have led to the characterization of thermally stable adsorbates during exposure of Pt(111) to benzene at low pressure ($<10^{-6}$ Torr) and low temperatures (<300 K). Among the most prominent techniques used are: low-energy electron diffraction (LEED),[18] near edge X-ray absorption spectroscopy (NEXAFS),[10] calorimetry,[6] thermal desorption spectroscopy,[7,12] electron energy loss spectroscopy (EELS),[9,19] and reflection−absorption infrared spectroscopy (RAIRS).[5,8] Density functional theory (DFT)[2−4] provides possible adsorption energies for different sites and chemical species. Taken together, the various techniques show benzene preferentially adsorbs to bridge sites in the low coverages limit whereas for high coverages adsorption onto 3-fold hollow sites is observed.[3] EELS studies display two distinct vibrational signatures in the cases of both low and high coverages, chemisorbed and physisorbed benzene.[19,20] The chemisorbed species is thought of as the dienyl benzene illustrated in Scheme 1, while physisorbed benzene is thought of as flat lying.[20,21]

SCHEME 1: Schematic Diagram of Dienyl Chemisorbed Benzene (C_6H_6) Intermediate

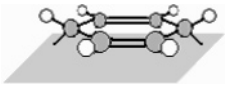

In this study, sum frequency generation (SFG) vibrational spectroscopy is employed to identify the surface intermediates during high-pressure (7.5, 10, 12.5, and 15 Torr) benzene reactions in the presence of hydrogen on Pt(111) at high temperatures (310−440 K). Under the electric dipole approximation, media with centrosymmetry and isotropic gases do not appear in the SFG spectrum. Bulk platinum has a center of inversion and its contribution to the SFG signal can therefore be neglected. At the surface, the symmetry is broken, giving rise to the surface specific signal. This explains why SFG is a more sensitive tool to study interfaces via vibrational spectroscopies in comparison to infrared absorption and Raman spectroscopies. Typically, electron spectroscopies cannot be employed under ambient pressure conditions necessary to perform catalytic reactions.

Here, we report evidence for chemisorbed dienyl benzene (C_6H_6) as the reactive surface intermediate for benzene hydrogenation on Pt(111) at high pressures (100 Torr H_2 with 7.5, 10, 12.5, and 15 Torr benzene and 10 Torr benzene with 10, 50, and 150 Torr H_2) and at high temperatures (310−440 K). At low temperatures we find that chemisorbed and physisorbed benzene coexist on the surface. This is the first study to show both chemisorbed and physisorbed benzene on Pt(111) simultaneously. At low pressures and temperatures, EELS studies of submonolayer coverages of benzene on Pt(111) produced chemisorbed dienyl benzene whereas saturation doses (1 langmuir) led to physisorption of the benzene.[20] Herein, we discuss the temperature- and pressure-dependent surface chemistry of benzene on Pt(111) in the presence of hydrogen.

* To whom correspondence should be addressed. Tel: 510-642-4053. Fax: 510-643-9668. E-mail: somorjai@socrates.berkeley.edu.

10.1021/jp0612735 CCC: $33.50
Published on Web 05/05/2006

2. Experimental Section

All experiments were carried out in a high pressure/ultrahigh vacuum (HP/UHV) system on a prepared Pt(111) single-crystal surface. The HP/UHV system consists of a UHV chamber operating at a base pressure of 2×10^{-9} Torr and a high-pressure (HP) cell isolated from the UHV chamber by a gate valve. The UHV chamber is equipped with an Auger electron spectrometer (AES), quadrupole mass spectrometer, and Ar^+ ion sputter gun. Two CaF_2 conflat windows on the HP cell allow transmission of infrared (IR), visible (vis), and sum frequency radiation for SFG experiments. The HP cell is equipped with a recirculation loop that includes a diaphragm pump and a septum for gas chromatographic analysis. The reactant and product gases are constantly mixed via a recirculation pump while kinetics data are acquired by periodically sampling the reaction mixture and measuring the relative gas-phase composition (FID detection and 0.1% AT-1000 on Graphpac GC 80/100 packed column (Alltech)).

The Pt(111) crystal was cleaned by sputtering with Ar^+ ions (1 keV) for 20 min, heating to 1123 K in the presence of 5×10^{-7} Torr O_2 for 2 min, and then annealing at 1123 K for 2 min. AES and LEED were used to verify the cleanliness of the Pt(111) surface after several cleaning cycles. The Pt(111) sample was then transferred into the HP cell for SFG reaction studies. Benzene (≥99.0%, EM Science) was purified by several freeze−pump−thaw cycles before introduction into the HP cell. Prior to the experiment, benzene was checked for impurities by means of GC. Such impurities were below 0.5% and consisted of mostly light alkanes below C_6.

A Nd:YAG laser (1064 nm fundamental having a 20 ps pulse width operating at a 20 Hz repetition rate) was used to create a tunable IR (1800−4000 cm^{-1}) and a second harmonic VIS (532 nm) beam. The VIS beam (200 μJ) and the IR (200 μJ) beams were spatially and temporally overlapped on the Pt(111) surface with incident angles of 55° and 60°, with respect to the surface normal. All spectra were taken using a ppp polarization combination (SFG, vis, and IR beams were all p-polarized). The generated SFG beam was sent through a monochromator, and the signal intensity was detected with a photomultiplier tube and a gated integrator as the IR beam was scanned over the range of interest. Spectra were curve fit using a previously reported procedure[22,23] to a form of the equation

$$I_{\mathrm{SFG}} \propto \left| \chi_{\mathrm{NR}}^{(2)} e^{i\phi_{\mathrm{NR}}} + \sum_q \frac{Aq}{\omega_{\mathrm{IR}} - \omega q + i\Gamma_q} e^{i\gamma_q} \right|^2 \qquad (1)$$

where $\chi_{\mathrm{NR}}^{(2)}$ is the nonresonant nonlinear susceptibility, $e^{i\phi_{\mathrm{NR}}}$ is the phase associated with the nonresonant background, A_q is the strength of the qth vibrational mode, ω_{IR} is the frequency of the incident infrared laser beam, ω_q is the frequency of the qth vibrational mode, Γ_q is the natural line width of the qth vibrational transition, and $e^{i\gamma_q}$ is the phase associated with the qth vibrational transition. Detailed descriptions on the HP/UHV system and SFG measurement can be found elsewhere.[11,13,24−27]

3. Results

3.1. Turnover Rates, Reaction Orders, and Activation Energies To Form the Products (Cyclohexane and Cyclohexene) under Varied Pressures of Benzene and Hydrogen on Pt(111). Figure 1 shows the kinetic data for 100 Torr of hydrogen and 7.5, 10, 12.5, and 15 Torr of benzene pressures, respectively, over a temperature range from 310 to 440 K.

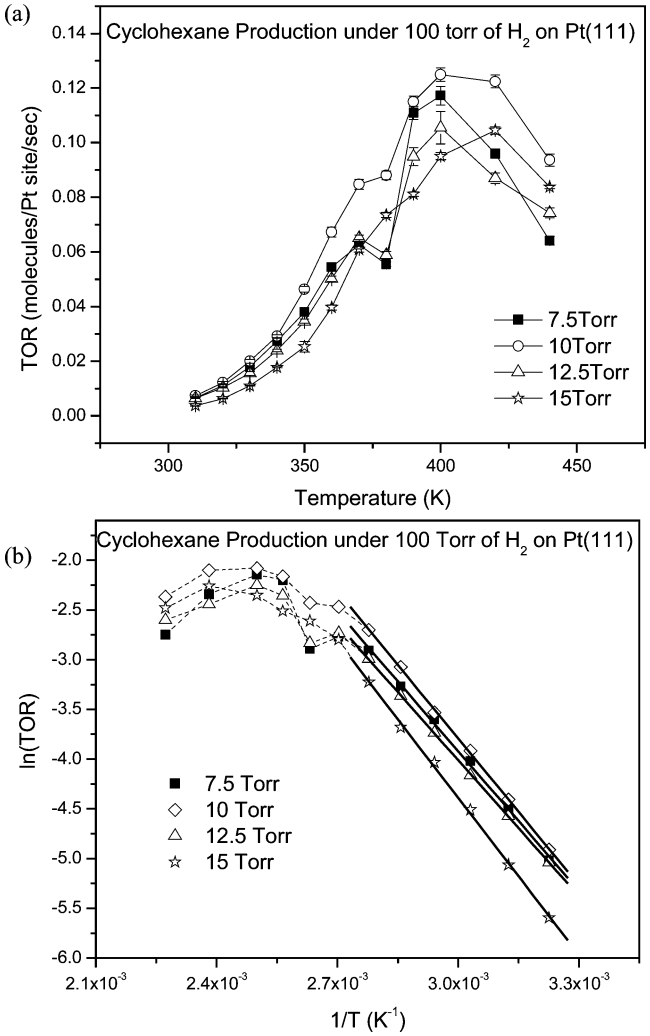

Figure 1. (a) Turnover rates (TORs), in molecules per Pt atom per second, for benzene (at 7.5, 10, 12.5, and 15 Torr) hydrogenation to cyclohexane in the presence of H_2 (100 Torr). (b) Arrhenius plots of the TORs. Apparent activation energies and preexponentials are listed in Table 1. The decrease in TOR at 380 K followed by a sharp increase at 390 K is attributed to the onset of cyclohexene production. (See Figure 2a.) Cyclohexene has a higher sticking probability on platinum resulting in further hydrogenation to cyclohexane. The non-Arrhenius behavior above 370 K is explained in terms of changes in the surface coverage of the adsorbates. Dotted lines are for visual aid.

Estimated turnover rates (TORs) (molecules Pt $site^{-1}$ s^{-1}) are shown in Figure 1a illustrating the production of cyclohexane at different temperatures. The TORs are calculated assuming that every platinum surface atom is an active site. Errors associated with these measurements are given as error bars. Arrhenius plots of the TORs are given in Figure 1b. This reaction also produces cyclohexene at higher temperatures. The TORs for cyclohexene formation are shown in Figure 2a along with the corresponding Arrhenius plots in Figure 2b. In a second experiment, the benzene pressure was held constant at 10 Torr and the H_2 pressure was adjusted to 10, 50, 100, and 150 Torr. The corresponding cyclohexane and cyclohexene TORs are shown in Figures 3a and 4a with the matching Arrhenius plots being displayed in Figures 3b and 4b, respectively. Above 370 and 420 K, the observed turnover rates for cyclohexane and cyclohexene deviate from the linear Arrhenius regression line. This is due to a change in the surface coverage of adsorbed species as previously discussed.[11] Apparent activation energies and preexponentials for cyclohexane and cyclohexene are listed in Tables 1 and 2. The apparent activation energies depend on

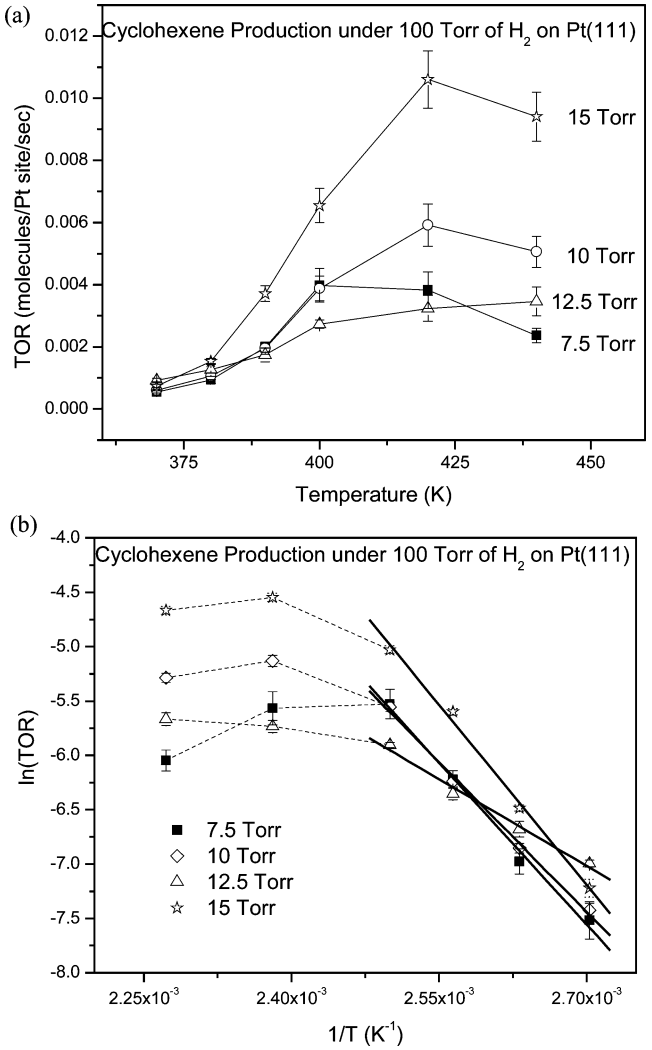

Figure 2. (a) Turnover rates (TORs), in molecules per Pt atom per second, for benzene (at 7.5, 10, 12.5, and 15 Torr) hydrogenation to cyclohexene in the presence of H_2 (100 Torr). (b) Arrhenius plots of the TORs. Apparent activation energies and preexponentials are listed in Table 2. The non-Arrhenius behavior above 420 K is explained in terms of changes in the surface coverage of the adsorbates. Dotted lines are for visual aid.

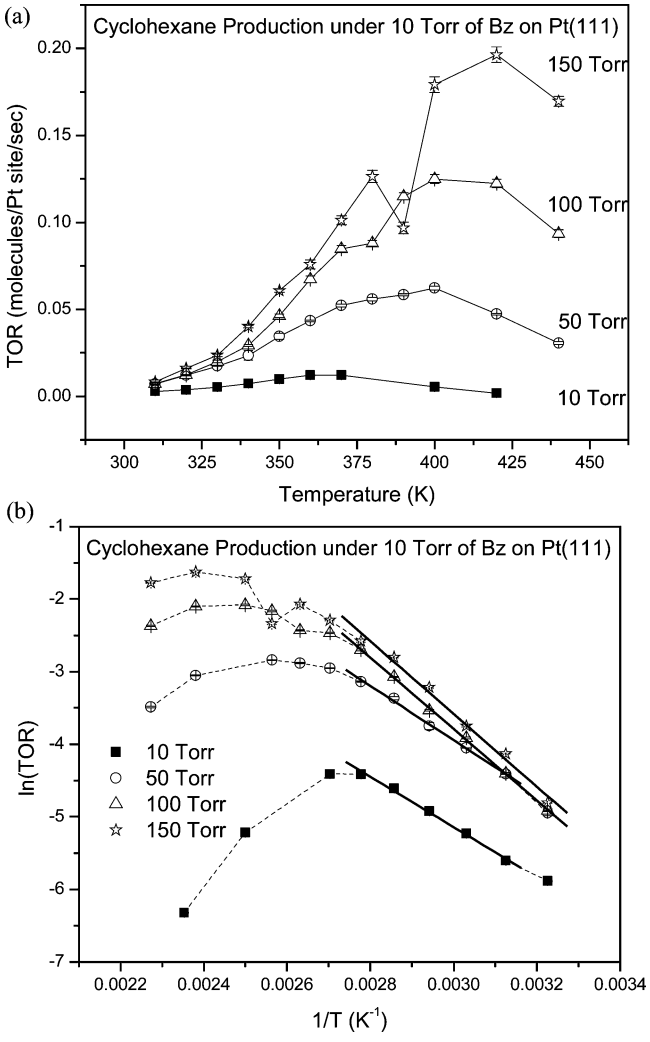

Figure 3. (a) Turnover rates (TORs), in molecules per Pt atom per second, for benzene (10 Torr) hydrogenation to cyclohexane in the presence of H_2 (at 10, 50, 100, and 150 Torr). (b) Arrhenius plots of the TORs. Apparent activation energies and preexponentials are listed in Table 1. The decrease in TOR at 380 K followed by a sharp increase at 390 K is attributed to the onset of cyclohexene production. (See Figure 4a.) Cyclohexene has a higher sticking probability on platinum resulting in further hydrogenation to cyclohexane. The non-Arrhenius behavior above 370 K is explained in terms of changes in the surface coverage of the adsorbates. Dotted lines are for visual aid.

the pressure of each reactant. In many hydrogenation reactions (e.g., ethylene, propylene, *n*-hexene, cyclohexene, etc.), H_2 is more strongly adsorbed than the hydrocarbon reactant and has a dominant effect on the apparent activation energies.[28] Benzene, in contrast, binds very strongly to the Pt(111) surface, and large changes in the apparent activation energies are expected upon varying its partial pressure. This change in activation energy is more noticeable in cyclohexene producing hydrogenation pathway as illustrated in Tables 1 and 2.

The rate law for benzene hydrogenation can be described by a standard empirical power law

$$r = kP_{\mathrm{Bz}}{}^{a}P_{\mathrm{H_2}}{}^{b} \tag{2}$$

where r is the rate of reaction, P_{Bz} and $P_{\mathrm{H_2}}$ are the pressures of the reactant gases (benzene and H_2, respectively), a and b are the reaction order with respect to the reactant species, and k is the rate constant. The rate constant can be expressed as

$$k = Ae^{-E_a/RT} \tag{3}$$

where A is the preexponential factor, E_a is the activation energy, R is the gas constant, and T is temperature. The exponents a and b are determined over a range of reaction temperatures (310−360 K for cyclohexane and 370−400 K for cyclohexene) using

$$a = \left[\frac{\partial \ln r}{\partial \ln P_{\mathrm{Bz}}}\right]_{P_{\mathrm{H_2}}} \tag{4}$$

The benzene and H_2 reaction orders for both cyclohexane and cyclohexene production are listed in Tables 1 and 2.

In Figures 1a and 3a, one observes a sharp dip in the reaction rate plot for cyclohexane formation at approximately 380 K. We assign this feature to the onset of cyclohexene formation. Cyclohexene formation is observed at 370 K but increases significantly above 390 K. Because of its larger sticking coefficient compared to cyclohexane (<0.1[6]), we expect cyclohexene (0.2[29]), once formed, to be an intermediate on the surface, which remains adsorbed until it is further hydrogenated to cyclohexane.

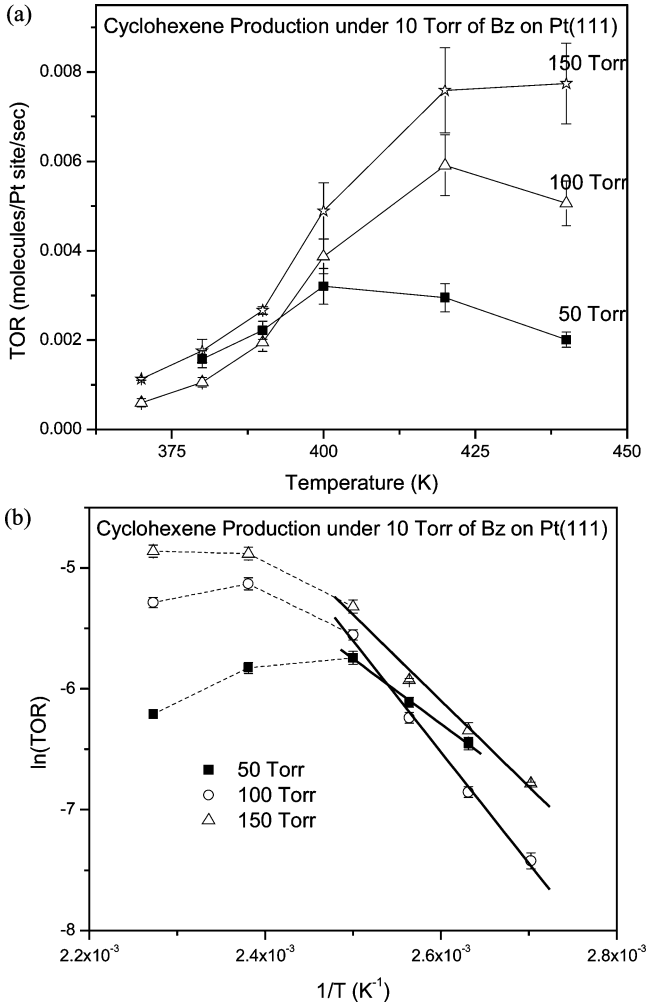

Figure 4. (a) Turnover rates (TORs), in molecules per Pt atom per second, for benzene (10 Torr) hydrogenation to cyclohexene in the presence of H_2 (at 50, 100, and 150 Torr). (b) Arrhenius plots of the TORs. Apparent activation energies and preexponentials are listed in Table 2. The non-Arrhenius behavior above 420 K is explained in terms of changes in the surface coverage of the adsorbates. Dotted lines are for visual aid.

3.2. Temperature Dependence of the Major Surface Species under Varied Pressures of Benzene and Hydrogen on Pt(111): SFG Vibrational Spectroscopy Results and Peak Assignments. SFG spectra of the surface species on Pt(111) at 15 Torr benzene and 100 Torr H_2 at various temperatures are shown in Figure 5. At 300 K, peaks are observed at 2945, 3030, and 3060 cm^{-1}. As the temperature is increased to 360 K, the peak intensity at 3060 cm^{-1} drops until it completely disappears at 400 K. The peaks at 2945 and 3030 cm^{-1}, on the other hand, increase over the temperature range from 310 to 420 K. Cooling the surface from 440 to 300 K reveals reversible behavior of the surface composition. The peak at 3060 cm^{-1} is assigned to physisorbed benzene.[19] Benzene has been shown to adsorb parallel to the Pt(111) surface by EELS,[19,20] NEXAFS,[10] RAIRS,[5] and DFT.[3,4] The molecule is still intact since it is physisorbed and the six carbons and hydrogens are assumed to be roughly equivalent giving rise to only one peak in the region the spectra were taken as observed by EELS.[19,20] Furthermore, gas-phase benzene exhibits an aromatic C−H stretch at 3068 cm^{-1}, which corresponds quite well to the surface vibrational spectra,[19] justifying the assignment of physisorbed benzene.

It becomes clear by comparison that the SFG spectra in Figure 5 are different from the SFG and RAIRS data of di-σ-type cyclohexene (C_6H_{10}), π-allyl c-C_6H_9, cyclohexyl (C_6H_{11}), and cyclohexadienes (C_6H_8). Literature on cyclic C_6 hydrocarbon chemistry on the Pt(111) surface will be used for comparing surface species found on the Pt(111) surface. The RAIRS[30] (SFG[31]) spectrum of di-σ-type cyclohexene on Pt(111) is distinguished by three bands at $\upsilon(CH_{2,distal}) = 2938$ (2958), $\upsilon_{asym}(CH_2) = 2902$ (2918), and $\upsilon_{sym}(CH_2) = 2864$ (2875) cm^{-1} of equal intensity. The RAIRS[30] (SFG[14]) spectrum of π-allyl c-C_6H_9 shows $\upsilon_{sym}(CH_2) = 2846$ (2845) and $\upsilon_{asym}(CH_2) = 2930$ (2925) cm^{-1}. The cyclohexyl SFG[15] spectrum exhibits two equally intense vibrational signatures at $\upsilon_{sym}(CH_2) = 2850$ and $\upsilon_{asym}(CH_2) = 2915$ cm^{-1}. The RAIRS[30] (SFG[31]) of 1,3-cyclohexadiene reveals modes at $\upsilon_{sym}(CH_2) = 2816$, $\upsilon_{sym}(CH_2) = 2825$ (2830), $\upsilon_{sym}(CH_2) = 2859$ (2875), and $\upsilon_{asym}(CH_2) = 2881$ (2900) cm^{-1}, and the relative intensities of the bands are again similar. Finally, the RAIRS[30] (SFG[31]) spectrum of 1,4-cyclohexadiene has only one mode at $\upsilon_{sym,sym}(CH_2) = 2763$ (2770) cm^{-1}. Presumably, the absence of a symmetric CH_2 stretch in Figure 5 indicates that the adsorbate is some C_6H_6 or more dehydrogenated species (e.g., polyaromatics).

TABLE 1: Preexponentials (in molecules per Pt atom per second), Apparent Activation Energies (in kcal/mol), Orders for Both H_2 and Benzene, Isokinetic Temperature (in K), and the Critical Vibration (in cm^{-1}) for Cyclohexane Production under a Constant Pressure of 10 Torr Benzene Varying H_2 and under Constant Pressure of 100 Torr H_2 while Varying Benzene

	$\ln(A$/molecules site^{-1} s$^{-1})$	E_a/(kcal mol^{-1})
	10.5 Torr Benzene	
11.2 Torr H_2	3.03 ± 0.33	6.95 ± 0.22
52 Torr H_2	4.71 ± 0.49	7.95 ± 0.33
105 Torr H_2	7.28 ± 0.14	9.81 ± 0.09
158 Torr H_2	8.52 ± 0.65	10.6 ± 0.4
	105 Torr H_2	
7.9 Torr Bz	6.02 ± 0.33	9.27 ± 0.35
10.5 Torr Bz	7.28 ± 0.14	9.81 ± 0.09
13.3 Torr Bz	5.92 ± 0.14	8.88 ± 0.12
16.5 Torr Bz	8.16 ± 0.65	10.5 ± 0.2
	T_i/(K)	ν/(cm^{-1})
CHA	317 ± 15	443 ± 22
		order
benzene		−1.1 ± 0.1
H_2		0.6 ± 0.01

TABLE 2: Preexponentials (in molecules per Pt atom per second), Apparent Activation Energies (in kcal/mol), Orders for Both H_2 and Benzene, Isokinetic Temperature (in K), and the Critical Vibration (in cm^{-1}) for Cyclohexene Production under a Constant Pressure of 10 Torr Benzene Varying H_2 and under Constant Pressure of 100 Torr H_2 while Varying Benzene

	$\ln(A$/molecules site^{-1} s$^{-1})$	E_a/(kcal mol^{-1})
	10.5 Torr Benzene	
52 Torr H_2	12.1 ± 0.6	10.7 ± 0.4
105 Torr H_2	21.4 ± 1.1	18.3 ± 0.8
158 Torr H_2	16.1 ± 1.4	14.1 ± 1.1
	105 Torr H_2	
7.9 Torr Bz	23.5 ± 1.5	19.7 ± 1.2
10.5 Torr Bz	21.4 ± 1.1	18.3 ± 0.8
13.3 Torr Bz	11.2 ± 1.1	10.6 ± 0.8
16.5 Torr Bz	25.4 ± 0.9	21.2 ± 0.7
	T_i/(K)	ν/(cm^{-1})
CHE	317 ± 15	443 ± 22
		order
benzene		-0.7 ± 0.1
H_2		0.6 ± 0.1

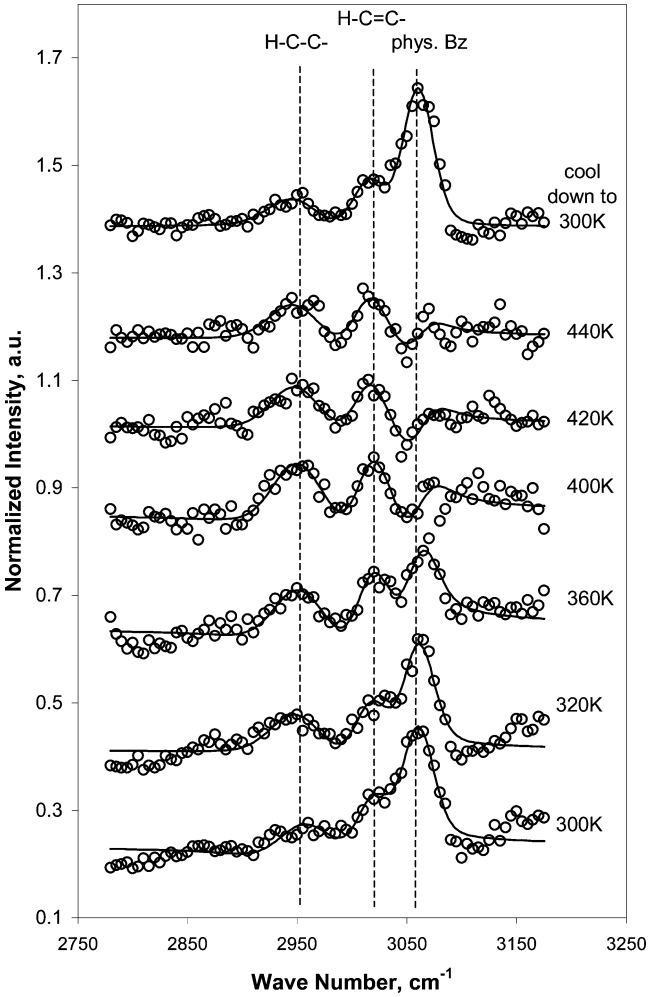

Figure 5. Temperature-dependent SFG spectra of surface species on Pt(111) under 15 Torr of benzene and 100 Torr H_2 in the range of 300−440 K. The top SFG spectrum was taken after the metal surface was cooled from 440 to 300 K. H−C−C−, vinylic (H−C═C−), and physisorbed benzene (phys. Bz) bands are identified. Markers represent experimental data and solid lines represent the curve fits.

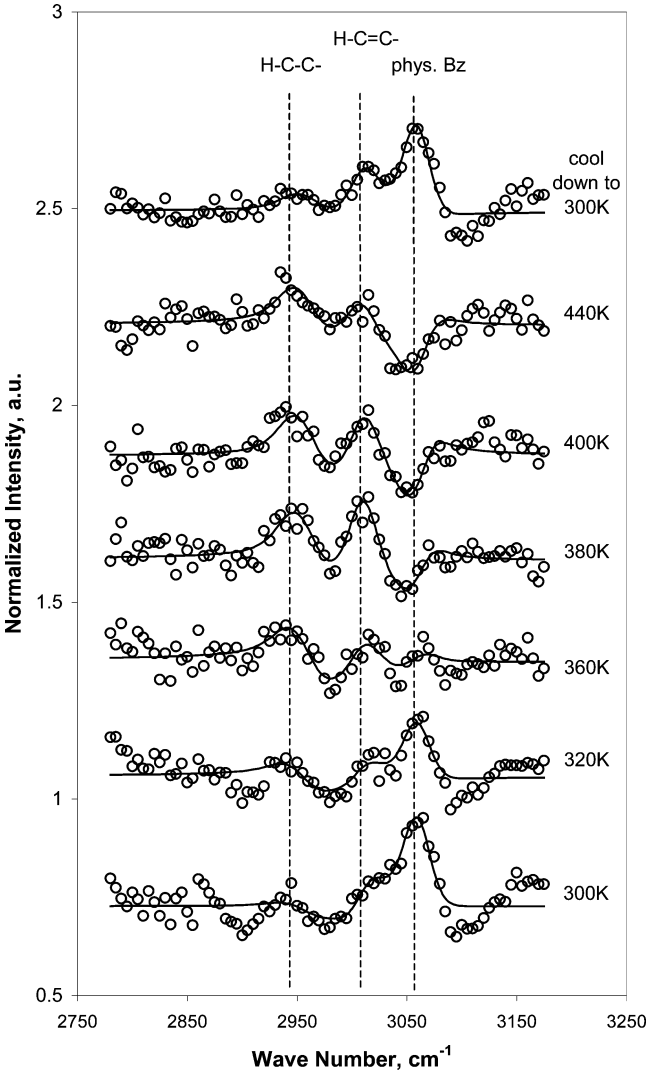

Figure 6. Temperature-dependent SFG spectra of surface species on Pt(111) under 7.5 Torr benzene and 100 Torr H_2 in the range of 300−440 K. The top SFG spectrum was taken after the metal surface was cooled from 440 to 300 K. H−C−C−, vinylic (H−C═C−), and physisorbed benzene (phys. Bz) bands are identified. Markers represent experimental data and solid lines represent the curve fits.

Previous infrared/high-resolution electron energy loss spectroscopy (IR/HREELS)[20,21] studies on benzene adsorption at low coverages (0.2 langmuir, 1 langmuir = 10^{-6} Torr·s) have revealed two peaks centered around 2960 and 3020 cm^{-1}. The 2960 cm^{-1} peak suggests the presence of some sp^3 hybridized carbon. Moreover, Thomas et al.[20] did not detect the presence of the 1815 and 1960 cm^{-1} peaks indicating that the adsorbed benzene is of a dienyl chemisorbed nature (see Chart 1). Grassian and Muetterties[21] have also presented a similar chemisorbed structure. According to those two groups, the adsorbate has six equivalent carbon−carbon bonds, two double and four single. The two singly bonded carbons are also bonded to the platinum surface, explaining the sp^3 hybridization character in the spectral signature. These results are further corroborated in Figure 5 by the apparent simultaneous growth and decay variation of the temperature. Hence, the modes in Figure 5 have been assigned as follows: υ(H−C−C−) = 2945 cm^{-1}, υ(C−H)(vinylic) = 3030 cm^{-1}, and υ(C−H)(aromatic) = 3060 cm^{-1}.

Figure 6 shows the SFG spectra of 7.5 Torr benzene and 100 Torr H_2 on Pt(111) as the temperature is varied. The results are strikingly similar to the previously discussed 15 Torr benzene case (Figure 5). Both chemisorbed and physisorbed benzene are observed at 300 K. The physisorbed benzene slowly desorbs as the surface temperature is increased to 360 K and vanishes completely at 400 K. Both peaks responsible for the chemisorbed benzene increase in intensity as the surface temperature is raised to 420 K. When the surface is allowed to cool, the physisorbed benzene, once again, becomes the dominant surface species displaying that the reaction is reversible.

Experiments on other pressure combinations (10 Torr benzene under 10, 50, 100, and 150 Torr H_2 and 12.5 Torr benzene under 100 Torr H_2) exhibited the same pattern of chemisorbed and physisorbed benzene coexisting on the platinum surface until the temperature was increased to 360 K, at which point only chemisorbed benzene is present. The chemisorbed dienyl has a maximum intensity at 420 K. Cooling the surface reverses the reaction resulting in physisorbed benzene being the dominant surface species.

4. Discussion

4.1. Compensation Effect and Isokinetic Temperature. The Arrhenius plots for both cyclohexane and cyclohexene production (Figures 1b, 2b, 3b, and 4b) have yielded apparent activation energies and preexponential factors for all pressure variations.

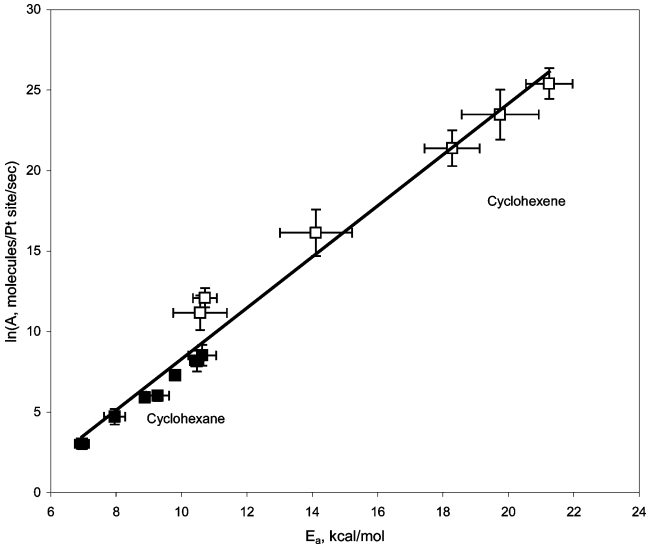

Figure 7. Constable plot for the hydrogenation of benzene to cyclohexane and cyclohexene. Open symbols represent cyclohexene and closed denote cyclohexane.

The resulting Arrhenius plot parameter pairs form a straight line, as presented in Figure 7, and exhibit compensation behavior. The isokinetic temperature is derived from the natural logarithm of eq 3

$$\ln A = \frac{E_a}{RT} + \ln k \tag{5}$$

and is related to the slope of the compensation effect. The isokinetic temperature (T_{iso}) is 317 ± 15 K for both cyclohexane and cyclohexene formation. This temperature seems to agree with the point at which the Arrhenius plots intersect. A possible explanation of the isokinetic temperature, as explained by Molinari,[32] is the existence of an equilibrium between adsorption and desorption at T_{iso}. An alternative model proposed by Larsson[33] is based on "selective energy transfer at the active site" which he further explains as a particular transfer of "energy into the vibrational mode of the reactant that most effectively takes the system to the activated state." Larsson[34] has treated the system as a "coupled, damped, oscillation system of classical physics" and derives the following equation

$$T_{iso} = NhcR^{-1}(\nu^2 - \omega^2)\omega^{-1}\left\{\pm\frac{1}{2}\pi - \arctan[0.5\nu\omega(\nu^2 - \omega^2)]^{-1}\right\}^{-1} \tag{6}$$

where υ is the vibrational mode leading toward reaction, ω is the frequency of the heat bath, N is Avogadro's number, h is Planck's constant, and c is the speed of light. For maximum efficacy of resonance energy transfer, $\omega = \upsilon$, eq 6 becomes

$$T_{iso} = \frac{Nhc}{2R\nu} = 0.719\nu \tag{7}$$

On the basis of the above equation, a critical frequency of vibration for cyclohexane and cyclohexene production is found to be 443 ± 22 cm^{-1}. This corresponds to a metal−carbon stretching vibrational mode,[19,20] which facilitates the $sp^2 \rightarrow sp^3$ reaction.

4.2. Kinetics and Suggested Reaction Pathways of Benzene Hydrogenation. Kinetic results have shown the formation of two products during the hydrogenation of benzene: cyclohexane and cyclohexene. The onset of cyclohexane production occurs at a lower temperature compared to that of cyclohexene. The surface concentration of cyclohexene, increases with temperature and is an endothermic process. However, both cyclohexane and cyclohexene production appear to be intimately tied with the dienyl chemisorbed benzene species since its peaks follow the rise and fall of the turnover rate (of both products) as the surface temperature is varied. This implies that there are at least two reaction mechanisms.

According to Koel et al.,[35] the most favorable pathway for benzene hydrogenation to cyclohexane occurs in a Horiuti−Polanyi mechanism[36] involving cyclohexene as an intermediate. The likely observable intermediates for this pathway would be η^5-cyclohexadienyl, π-allyl c-C_6H_9, and di-σ cyclohexene. As stated previously, these species are unlikely to be on the platinum surface at high pressures since the absence of symmetric CH_2 modes indicates that the molecule does not have any CH_2 groups. Furthermore, chemisorbed benzene is not likely to be an abundant surface intermediate for this pathway since adsorbed benzene immediately hydrogenates to η^5-cyclohexadienyl.

Saeys et al.[3] have developed another possible reaction pathway via DFT. Instead of using chemical intuition to determine a rate-determining step and pathway, 14 possible reaction paths were proposed for the six sequential hydrogenation steps. The dominant pathway does not proceed through cyclohexene, as Koel et al.[35] have proposed, favoring this as the most probable mechanism for benzene hydrogenation to cyclohexane at low temperatures. Saeys et al.[3] also conclude that "the thermodynamic sink of the energy profile is clearly the adsorbed benzene and hydrogen. They are likely to be the most-abundant reaction intermediates." Adsorbed benzene in the "thermodynamic sink" may be attributed to dienyl chemisorbed benzene, as proposed based on the SFG results in Figures 5 and 6, a finding which is consistent with the mechanism proposed by Saeys et al.[3] However, there is no spectroscopic evidence of any hydrogenated benzene species confirming the plausibility of this pathway, probably due to the short lifetime and small coverages of such species. In the DFT study presented by Saeys et al.[3], it was assumed that benzene adsorbs on the 3-fold hollow site; this seems preferable at low temperatures and coverages.[4] Higher temperatures favor the bridge site,[37] which, in this work, we assumed to correspond to the dienyl-type chemisorbed benzene. Bonding type effects (bridge versus 3-fold hollow) are not explored in the mechanism proposed by Saeys et al.[3]

The previously mentioned compensation effect indicates that the critical vibrational frequencies at 443 ± 22 cm^{-1} for cyclohexane and cyclohexene production could be attributed to a metal−carbon stretch, thus facilitating the $sp^2 \rightarrow sp^3$ reaction. In addition, Thomas et al.[20] have reported a vibrational mode for chemisorbed benzene at 475 cm^{-1}, which was assigned to metal−carbon stretches. The metal−carbon stretching frequency for physisorbed benzene was reported at 550 cm^{-1}, excluding the physisorbed species as the reactive intermediate by this model. The suggested structure for the dienyl species is clearly the product of the $sp^2 \rightarrow sp^3$ reaction and is likely to be the reactive surface intermediate in the benzene hydrogenation for both cyclohexane and cyclohexene.

5. Conclusions

We have identified surface intermediates at various temperatures during high-pressure catalytic reactions of benzene on Pt(111) using SFG surface vibrational spectroscopy. Chemi-

sorbed and physisorbed benzene were found to coadsorb at 310 K. Heating to 360 K made the physisorbed species disappear and resulted in only chemisorbed benzene on the surface. At 400 K the coverage of chemisorbed benzene reaches a maximum and decays as the temperatures is further raised to 440 K. When the surface was subsequently cooled from 440 to 310 K, the observed SFG spectrum was identical to that obtained before reaction indicating complete reversibility of the surface composition. Kinetic studies identified chemisorbed dienyl benzene as a possible critical vibration intermediate to form cyclohexane and cyclohexene. Resonance vibrational frequencies were extracted from the isokinetic temperature and agreed reasonably well with ones expected from a dienyl benzene-type surface species. To conclude, chemisorbed dienyl benzene is a reactive surface intermediate during benzene hydrogenation.

Acknowledgment. We thank Professor Ragnar Larrson for many discussions of the compensation effect and isokinetic temperature. This work was supported by the Director, Office of Energy Research, Office of Basic Energy Sciences, and Materials Science Division of the U.S. Department of Energy under Contract DE-AC02-05CH11231.

References and Notes

(1) Cooper, B. H.; Donnis, B. B. L. *Appl. Catal. A* **1996**, *137*, 203.
(2) Saeys, M.; Reyniers, M.; Marin, G. B.; Neurock, M. *Surf. Sci.* **2002**, *513*, 315.
(3) Saeys, M.; Reyniers, M.; Marin, G. B. *J. Phys. Chem. B* **2002**, *106*, 7489.
(4) Morin, C.; Simon, D., Sautet, P. *J. Phys. Chem. B* **2004**, *108*, 5653.
(5) Haq, S.; King, D. A. *J. Phys. Chem.* **1996**, *100*, 16957.
(6) Ihm, H. A., H. M.; Gottfried, J. M.; Bera, P.; Campbell, C. T. *J. Phys. Chem. B* **2004**, *108* (38), 14627.
(7) Lutterloh, C.; Biener, L.; Pohlmann, K.; Schenk, A.; Kuppers, J. *Surf. Sci.* **1996**, *352*−*354*, 133.
(8) Haaland, D. M. *Surf. Sci.* **1981**, *102*, 405.
(9) Abon, M.; Bertolini, J. C.; Billy, J.; Massardier, J.; Tardy, B. *Surf. Sci.* **1985**, 162, 395.
(10) Horsley, J. A.; Stohr, J.; Hitchcock, A. P.; Newbury, D. C.; Johnson, A. L.; Sette, F. *J. Chem. Phys.* **1985**, *83* (12), 6099.
(11) Bratlie, K. M.; Flores, L. D.; Somorjai, G. A. *Surf. Sci.* **2005**, *599*, (1−3), 93.
(12) Tsai, M.-C.; Muetterties, E. L. *J. Am. Chem. Soc.* **1982**, *104*, 2534.
(13) Yang, M.; Tang, D. C.; Somorjai, G. A. *Rev. Sci. Instrum.* **2003**, *74*, 4554.
(14) Yang, M.; Chou, K. C.; Somorjai, G. A. *J. Phys. Chem. B* **2003**, *107*, 5267.
(15) Yang, M.; Somorjai, G. A. *J. Am. Chem. Soc.* **2003**, *125*, 11131.
(16) Yang, M.; Chou, K. C.; Somorjai, G. A. *J. Phys. Chem. B* **2004**, *108*, 14766.
(17) Yang, M.; Dunietz, B.; Head-Gordon, M.; Somorjai, G. A. In publication.
(18) Ogletree, D. F.; Van Hove, M. A.; Somorjai, G. A. *Surf. Sci.* **1987**, *183*, 1.
(19) Lehwald, S.; Ibach, H.; Demuth, J. E. *Surf. Sci.* **1978**, *78*, 577.
(20) Thomas, F. S.; Chen, N. S.; Ford, L. P.; Masel R. I. *Surf. Sci.* **2001**, *486*, 1.
(21) Grassian, V. H.; Muetterties, E. L. *J. Phys. Chem.* **1987**, *91*, 389.
(22) Bain, C. D.; Davies, P. B.; Ong, T. H.; Ward, R. N.; Brown, M. A. *Langmuir* **1991**, *7*, 1563.
(23) Moore, F. G.; Becraft, K. A.; Richmond, G. L. *Appl. Spectrosc.* **2002**, *56*, 1575.
(24) Kung, K. Y.; Chen, P.; Wei, F.; Rupprechter, G.; Shen, Y. R.; Somorjai, G. A. *Rev. Sci. Instrum.* **2001**, *72*, 1806.
(25) Shen, Y. R. *The Principles of Nonlinear Optics*; Wiley: New York, 2003.
(26) Shen, Y. R. *Annu. Rev. Phys. Chem* **1989**, *40*, 327.
(27) Shen, Y. R. *Nature* **1989**, *337*, 519.
(28) Bond, G. C.; Keane, M. A.; Kral, H.; Lercher, J. A. *Catal. Rev.* **2000**, *42* (3), 323.
(29) Henn, F. C.; Diaz, A. L.; Bussel, M. E.; Huggenschmidt, M. B.; Domagala, M. E.; Campbell, C. T. *J. Phys. Chem.* **1992**, *96*, 5965.
(30) Manner, W. L.; Girolami, G. S.; Nuzzo, R. G. *J. Phys. Chem. B* **1998**, *102*, 10295.
(31) Su, X.; Kung, K.; Lahtinen, J.; Shen, R. Y.; Somorjai, G. A. *J. Mol. Catal. A* **1999**, *141*, 9−19.
(32) Molinari, E. *Z. Phys. Chem.* **1956**, *6*, 1.
(33) Larsson, R. *Catal. Today* **1987**, *1*, 93.
(34) Lomot, D.; Juszczyk, W.; Karpinski, Z.; Larsson, R. *J. Mol. Catal. A* **2002**, *186* (1−2), 163.
(35) Koel, B. E.; Blank, D. A.; Carter, E. A. *J. Mol. Catal. A*: *Chem.* **1998**, *131*, 39−53.
(36) Horiuti, J.; Polanyi, M. *Trans. Faraday Soc.* **1934**, *30*, 1164.
(37) Weiss, P. S.; Eigler, D. M. *Phys. Rev. Lett.* **1993**, *71*, (19), 3139.